



# Integrated approach for enhanced bio-oil recovery from disposed face masks through co-hydrothermal liquefaction with *Spirulina platensis* grown in wastewater

Li Li<sup>1</sup> · Jin Huang<sup>1</sup> · Adel W. Almutairi<sup>2</sup> · Xin Lan<sup>1</sup> · Linling Zheng<sup>1</sup> · Yuling Lin<sup>1</sup> · Liudong Chen<sup>1</sup> · Nanjie Fu<sup>1</sup> · Zongren Lin<sup>1</sup> · Abd El-Fatah Abomohra<sup>1</sup>

Received: 7 July 2021 / Revised: 12 August 2021 / Accepted: 26 August 2021 / Published online: 25 September 2021  
© The Author(s), under exclusive licence to Springer-Verlag GmbH Germany, part of Springer Nature 2021

## Abstract

Currently, the enormous generation of contaminated disposed face masks raises many environmental concerns. The present study provides a novel route for efficient crude bio-oil production from disposed masks through co-hydrothermal liquefaction (Co-HTL) with *Spirulina platensis* grown in wastewater. Ultimate and proximate analysis confirmed that *S. platensis* contains relatively high nitrogen content (9.13 %dw), which decreased by increasing the mask blend ratio. However, carbon and hydrogen contents were higher in masks (83.84 and 13.77 %dw, respectively). In addition, masks showed 29.6% higher volatiles than *S. platensis*, which resulted in 94.2% lower ash content. Thermal decomposition of masks started at a higher temperature ( $\approx 330$  °C) comparing to *S. platensis* ( $\approx 208$  °C). The highest bio-oil yield was recorded by HTL of *S. platensis* and Co-HTL with 25% (w/w) masks at 300 °C, which showed insignificant differences with each other. GC/MS analysis of the bio-oil produced from HTL of algal biomass showed a high proportion of nitrogen- and oxygen-containing compounds (3.6% and 11.9%, respectively), with relatively low hydrocarbons (17.4%). Mask blend ratio at 25% reduced the nitrogen-containing compounds by 55.6% and enhanced the hydrocarbons by 43.7%. Moreover, blending of masks with *S. platensis* enhanced the compounds within the diesel range in favor of gasoline and heavy oil. Overall, the present study provides an innovative route for enhanced bio-oil production through mask recycling coupled with wastewater treatment.

**Keywords** Biofuel · COVID-19 · Medical wastes · Microalgae · Waste to energy

## 1 Introduction

In response to the outbreak of coronavirus (COVID-19) detected in December 2019, the World Health Organization declared the global pandemic situation in March 2020. By April 2021, more than 146 million cases have been confirmed globally, with about 3 million death [1]. Frequent countermeasures have been undertaken to control and

prevent the fatal pandemic [2, 3]. Wearing face masks plays a vital role to control and prevent infection, and it should not be abandoned [4]. This resulted in a sharp increase in the global demand for face masks, with an estimation of 129 billion masks per month [5]. Most disposed masks have high risk of contamination with coronavirus, as the virus can exist on many surfaces for few days. The pathogens in waste disposed masks, without proper treatments, can transmit the infection again to the public [6, 7] and have the potential to spread the virus [8]. In addition, disposable face masks have been identified as an emerging source of microplastic in the ecosystem, with many negative environmental impacts [9–11]. Therefore, disposed masks require an effective and proper treatment in order to help in disease containment and to save the ecosystem [12].

Disposed masks should be separately handled to prevent them from integration with the regular municipal waste. For treatment, incineration is one of the most common methods that can be used to treat disposed masks. The

✉ Jin Huang  
huangjin\_cd@cdu.edu.cn

✉ Abd El-Fatah Abomohra  
abomohra@cdu.edu.cn

<sup>1</sup> Department of Environmental Engineering, School of Architecture and Civil Engineering, Chengdu University, Chengdu 610106, China

<sup>2</sup> Biological Sciences Department, Faculty of Science & Arts, King Abdulaziz University, Rabigh, Saudi Arabia

process takes place at high temperatures and, therefore, it is more effective to kill pathogens compared to other physical and chemical methods [13]. However, it has many disadvantages such as toxins release into the environment which severely affect the immune system of humans and animals [9, 14, 15]. Thus, there is an urgent timely need to explore alternative eco-friendly technologies for disposed masks treatment. It is difficult to establish a reliable recycle platform for disposed masks due to the heterogeneous nature of mask materials, containing polypropylene, polyethylene, polystyrene, polyethylene terephthalate, and polyvinyl chloride [9, 16, 17]. Thermochemical conversion is one of the promising methods for mask degradation and conversion. However, efficient conversion of plastic wastes, including masks, requires high temperature. Therefore, co-conversion with other feedstocks would provide the advantages of high oil yield at relatively lower temperature. In that context, thermal co-conversion of plastics with biomass has been recommended to increase the quantity of the bio-oil and improve its quality [18–20].

Among different biomass feedstocks and comparing to woody biomass, thermochemical conversion of algae was reported to produce a comparable amount of bio-oil [21]. In addition, microalgae have many advantages over other feedstocks such as high growth rate, CO<sub>2</sub> sequestration, and wastewater treatment. Recently, *Spirulina platensis* has been discussed for high biomass production integrated with different applications [22–24]. However, biofuel production from *S. platensis* has limited large-scale application due to the elevated cost of microalgal cultivation, where about 80% of the total process costs are associated with nutrients and freshwater consumption [25]. Application of wastewater as a growth medium to provide the microalgae with nutrients has significant environmental and economic potentials to produce the biomass at low cost coupled with wastewater treatment [26, 27]. Nevertheless, disposal of contaminated biomass represents a challenge for process commercialization, where biofuel production was discussed as a prominent route [28]. Among different thermochemical conversion methods, hydrothermal liquefaction (HTL) is an advantageous conversion route for microalgae to avoid the drying step, due to decomposition of the whole biomass in hot compressed water [29, 30]. Although few recent studies evaluated the thermochemical conversion of disposed masks, Co-HTL of masks with other feedstocks was not previously evaluated. Therefore, the present study provides a feasible and effective proposal to one of the current challenges encountered during COVID-19 pandemic, aiming at efficient management of disposed masks. The study suggests a novel integrated strategy for industrial wastewater treatment by microalgae and enhanced bio-oil recovery through Co-HTL of waste disposable masks with microalgal biomass.

## 2 Materials and methods

### 2.1 Microalgae cultivation

*Spirulina platensis* was preserved axenically by frequent cultivation in 50 mL of Zarrouk medium [31]. Exponentially grown culture was used as inoculum for the experimental cultures using 50-cm × 7.5-cm glass photobioreactor cylinders. Each tube of the reactor contained 1.5 L of sterilized synthetic wastewater (SWW, Table S1) as modified from Zhai et al. [26] at initial OD<sub>560</sub> of 0.15 ± 0.02. A stock copper solution (1 g L<sup>-1</sup>) was prepared by dissolving copper sulfate in distilled water, then Cu<sup>2+</sup> concentration in the medium was adjusted at 10 mg L<sup>-1</sup> for Cu-enriched medium. All inoculated cultures were incubated at 25 ± 1 °C for 22 days under average light intensity of 70 μmol photons m<sup>-2</sup> s<sup>-1</sup> and a photoperiod of 18:6 h light:dark cycle. Aeration was performed using filtered air injected at the bottom of each culture vessel through a thin aeration tube. pH was adjusted at 8.5 using a pH controller (AquaMedic, Germany) by controlling the CO<sub>2</sub> supply. Each tube was covered with a rubber plug containing a hypodermic needle to allow gas exhaust. To enhance the growth and copper removal, 30 mT of static magnetic field (SMF) was applied for 6 h day<sup>-1</sup> as described by Shao et al. [32] and compared with a control culture without SMF application.

### 2.2 Biomass assay

#### 2.2.1 Growth

The growth was measured spectrophotometrically at 2-day interval by monitoring the optical density at 560 nm (OD<sub>560</sub>). In addition, the dry weight (dw) was determined at the late exponential phase (*Exp<sub>L</sub>*) and stationary phase (*Sta*). Biomass productivity was calculated using Eq. 1 [33]:

$$\text{Biomass productivity}(\text{gL}^{-1}\text{d}^{-1}) = (dw_t - dw_i) / \Delta t \quad (1)$$

where  $dw_t$  and  $dw_i$  represent the dry weight at the measured time ( $t$ ) and that at the start of culture, respectively, while  $\Delta t$  represents the time interval in days.

#### 2.2.2 Biomass composition

The main macromolecules in the biomass including carbohydrates, proteins, and lipids were determined after harvest by centrifugation for 10 min at 3000 ×  $g$ . Cellular proteins and carbohydrates were extracted by adding 10 mL of 1 N NaOH to the cell pellet and incubating for 2 h in a boiling water bath [34]. The concentration of total carbohydrates in the NaOH extract was measured using phenol–sulfuric acid method [35], while protein concentration was measured according

to the Bradford method [36]. Lipid extraction was carried out by adding 15 mL of chloroform:methanol (2:1, v/v) to the cell pellet followed by incubation at room temperature with shaking for 2 h, then 3 mL of 0.9% NaCl was added [37]. After centrifugation at  $200\times g$  for 2 min, the lower chloroform phase was siphoned and solvent was evaporated, the extracted lipids were dried at  $60\text{ }^{\circ}\text{C}$  for 30 min, then lipid amount was determined gravimetrically.

### 2.3 Biosorption analysis

Copper was determined in the grown culture at 4-day interval. Briefly, 10 mL of the culture was centrifuged at  $3000\times g$  for 10 min, then the liquid phase was filtered through 0.45- $\mu\text{m}$  pore-size filter to ensure cell separation. The filtrate was further analyzed spectrophotometrically for residual copper using sodium diethyldithiocarbamate [38].

### 2.4 Algae-mask blends

Because SMF treatment showed higher biomass yield and copper removal, it was applied to a 160-L tubular photobioreactor. *S. platensis* was harvested at  $Exp_L$  by flocculation using ferric chloride according to Sossella et al. [39]. The sludge was further centrifuged for 10 min at  $3000\times g$  to obtain the biomass, which was oven dried at  $105\text{ }^{\circ}\text{C}$  until constant weight. The dried biomass was ground and kept in vacuumed bags for further use, where distilled water was added before use (Section 2.6).

Disposable medical masks were purchased from the local market and collected after personal use by the ZhiXue research team at Chengdu University. After oven drying at  $105\text{ }^{\circ}\text{C}$  for 24 h, the different parts of masks were determined by weight (Fig. 1A). The whole disposed masks were cut into 0.2–0.5-mm pieces and blended with *S. platensis* in five ratios (0, 25, 50, 75, and 100%), where 0% and 100% represent the individual *S. platensis* and masks, respectively.

### 2.5 Blend characteristics

The contents of carbon, hydrogen, nitrogen, and sulfur, in the five blends were determined by CHNS analyzer (Elementar vario ELIII, Germany) and the results were expressed on a dry weight basis. Proximate analysis was performed according to ASTM E870-82 standard test methods [40]. Oxygen and fixed carbon were calculated by difference as described previously [41]. Thermogravimetric analyzer (STA449F-5, NETZSCH-Gerätebau GmbH, Germany) was used to determine the pattern of mass loss per elevated temperature up to  $1000\text{ }^{\circ}\text{C}$  at a heating rate of  $20\text{ }^{\circ}\text{C min}^{-1}$ . Higher heating values (HHVs,  $\text{MJ kg}^{-1}$ ) was calculated using Eq. 2 [42]:

$$HHV = 0.3403C + 1.2432H + 0.0628N + 0.1909S - 0.0984O \quad (2)$$

### 2.6 Hydrothermal (co-)liquefaction

Liquefaction experiments were carried out in a stainless-steel high-pressure reactor (Fig. 1B) following the experimental procedures shown in Fig. 2. Briefly, 2 g dw feedstock was mixed with distilled water (1:3, w/v), then loaded into the reactor, and 18 mL of 50% ethanol was added [43]. The reactor was tightly closed and heated up to the desired temperature at a heating rate of  $10\text{ }^{\circ}\text{C min}^{-1}$ . The reaction was carried out for 45 min with stirring at 500 rpm, then the reactor was cooled down in a water bath. The HTL products were rinsed from the reactor using dichloromethane (DCM), then the slurry was vacuum filtered to separate the solid portion, which was dried in an oven at  $105\text{ }^{\circ}\text{C}$  to obtain the biochar. DCM was evaporated in an oven at  $65\text{ }^{\circ}\text{C}$  to obtain the bio-oil. Gas and water-soluble products were summed together and presented as “WSG.” The yields of different products and conversion ratio were calculated using Eqs. 3–6:

$$\text{Bio - oil yield } (Y_{\text{oil}}, \%) = (M_{\text{oil}}/M_{\text{feed}}) \times 100 \quad (3)$$

$$\text{Bio - char yield } (Y_{\text{char}}, \%) = (M_{\text{char}}/M_{\text{feed}}) \times 100 \quad (4)$$

$$\text{WSG } (\%) = 100 - (Y_{\text{oil}} + Y_{\text{char}}) \quad (5)$$

$$\text{Conversion ratio } (\%) = 100 - Y_{\text{char}} \quad (6)$$

where  $M_{\text{feed}}$ ,  $M_{\text{oil}}$ , and  $M_{\text{char}}$  are the weights of injected feedstock, bio-oil, and biochar, respectively.

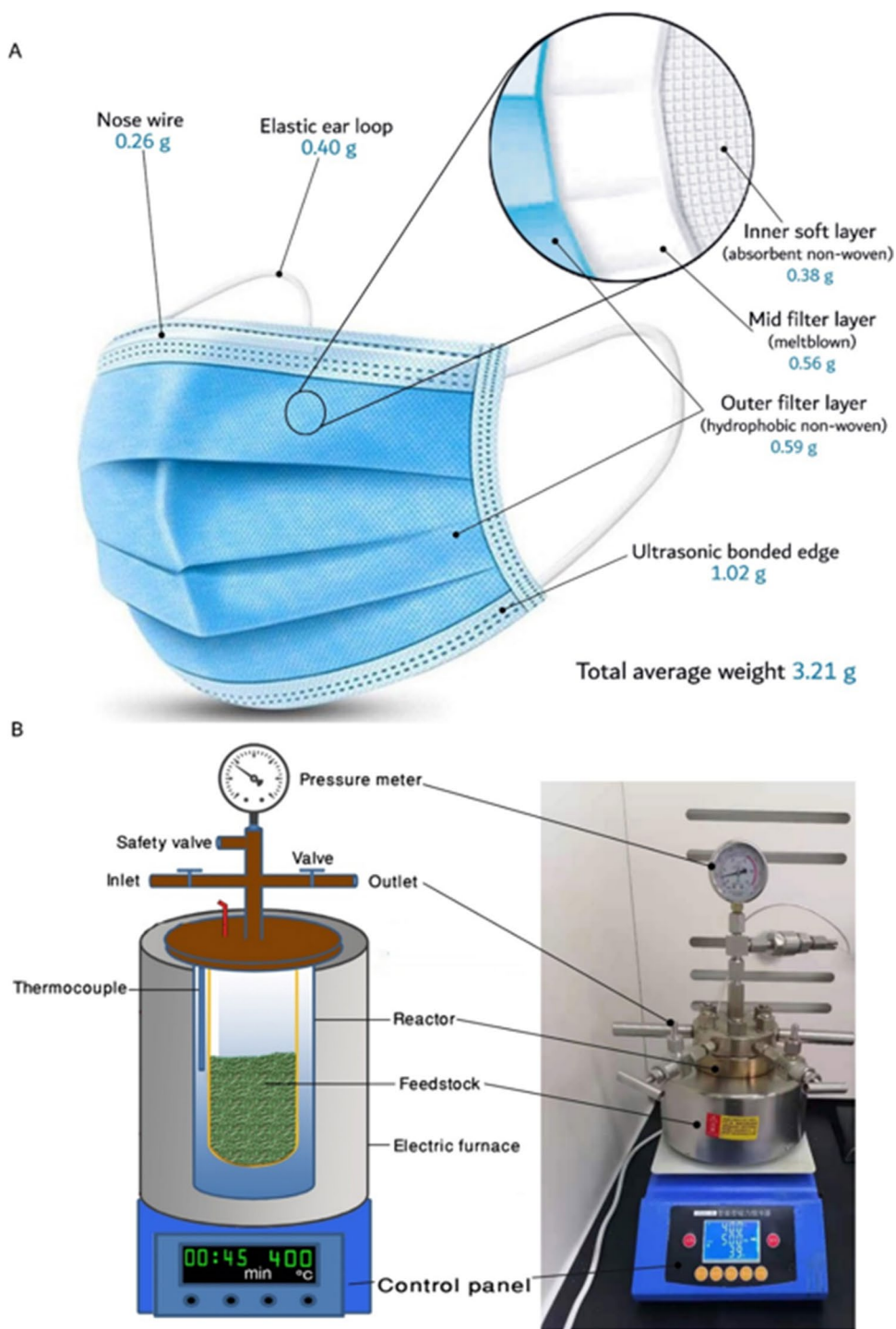
### 2.7 Bio-oil analysis

The bio-oil chemical composition was determined by gas chromatography-mass spectroscopy (GC/MS, QP2010PLUS, Shimadzu, Japan) coupled with an Agilent 5975C mass spectrometer. A volume of 1  $\mu\text{L}$  sample was injected, and oven temperature started at  $40\text{ }^{\circ}\text{C}$  where it was held for 5 min, then increased to  $290\text{ }^{\circ}\text{C}$  at a heating rate of  $5\text{ }^{\circ}\text{C min}^{-1}$ , where it was held for 15 min. Helium was used as a carrier gas at a flow rate of  $1\text{ mL min}^{-1}$ . Mass spectrum was operated at  $220\text{ }^{\circ}\text{C}$  under electron ionization of 70 eV and mass scan range  $m/z$  33–500 amu.

### 2.8 Statistical analysis

All experiments were carried out in three replicates and results are presented as the mean  $\pm$  standard deviation. One-way analysis of variance (ANOVA) followed by least significant difference (LSD) test at probability level ( $P$ )  $\leq 0.05$  was carried out by SPSS (IBM v.20) to determine the significant differences.

**Fig. 1** The different parts showing average weight of the used disposable masks (A), and schematic diagram showing the main parts of the used hydro-thermal liquefaction reactor (B)



### 3 Results and discussion

#### 3.1 Biomass and biochemical composition

To obtain more reliable results by maintaining stable microalgal cultivation in the present study, synthetic wastewater was utilized as a growth medium. The effect of SMF on growth and biochemical composition of *S. platensis* was

initially evaluated. Application of SMF up to 22 days stimulated the algal cell density by 17.8% higher than the untreated culture (Fig. 3). For SMF-treated culture, biomass productivity dropped sharply from day 16 to day 22 by 27.7% (Fig. 3), which is attributed to the reduction of growth rate by increasing the incubation time. For both cultures, day 16 and day 20 were considered as  $Exp_L$  and  $Sta$ , respectively. In addition, SMF-treated cultures showed 33.3% and 20.0%



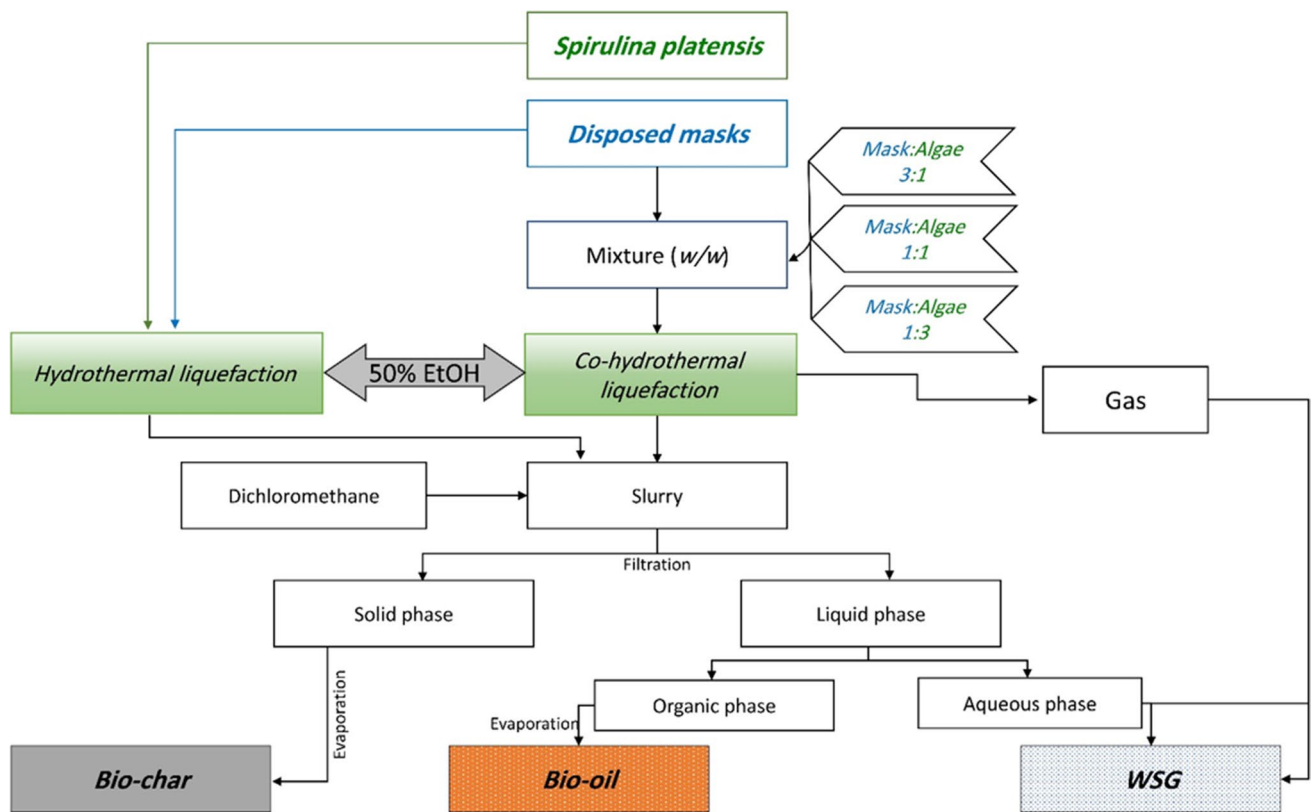
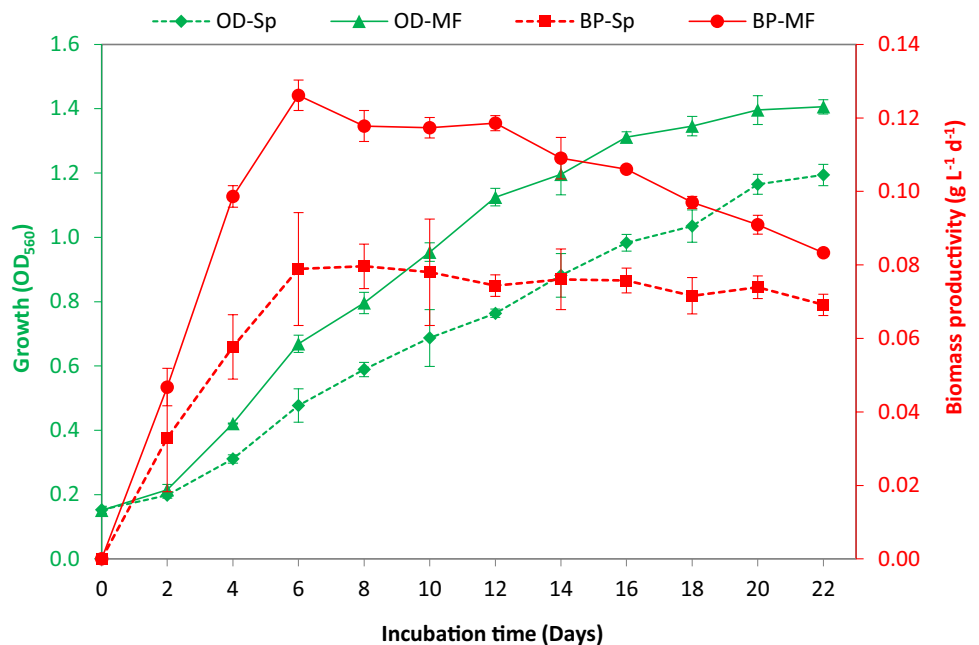


**Fig. 2** Experimental flow chart showing the procedures of (co-)hydrothermal liquefaction and product separation including biochar, bio-oil, and water-soluble compounds+ gas (WSG)

higher dry weight at  $Exp_L$  and  $Sta$ , respectively (Table 1). The maximum dry weight in the present study was  $2.04 \text{ g L}^{-1}$ , which is comparable to the results of Zhai et al. [26]

for *S. platensis* cultivated in SWW. However, it is 45.7% lower than that recorded for *S. platensis* cultivated in a specific *Spirulina* medium under the same SMF conditions

**Fig. 3** Growth (OD) and biomass productivity (BP) of *Spirulina platensis* grown in synthetic wastewater (Sp) and under static magnetic field (MF)



[32]. Thus, biomass production could be further enhanced by enrichment of SWW with more nutrients, which needs further optimization. Due to enhancement of growth, the SMF-treated culture showed  $0.106 \text{ g L}^{-1} \text{ day}^{-1}$  biomass productivity at  $Exp_L$ , which was 39.5% higher than that of the corresponding control (Table 1). It can be noted that SMF enhanced total carbohydrate content in favor of lipids, with slight changes in protein content (Table 1). This finding is in agreement with previous studies for optimization of SMF treatment on *S. platensis* [32], suggesting that SMF application is more suitable for enhanced bioethanol production than biodiesel.

**Table 1** Biomass and macromolecules of *Spirulina platensis* grown in synthetic wastewater (Sp) and under static magnetic field (MF) for 16 days ( $Exp_L$ ) and 20 days ( $Sta$ )

Parameters	Phase	Sp	MF
Dry weight ( $\text{g L}^{-1}$ )	$Exp_L$	$1.44 \pm 0.038$	$1.92 \pm 0.024^*$
	$Sta$	$1.70 \pm 0.045$	$2.04 \pm 0.066^*$
Biomass productivity ( $\text{g L}^{-1} \text{ day}^{-1}$ )	$Exp_L$	$0.076 \pm 0.002$	$0.106 \pm 0.001^*$
	$Sta$	$0.074 \pm 0.003$	$0.091 \pm 0.002^*$
Carbohydrates (%dw)	$Exp_L$	$15.52 \pm 0.387$	$23.65 \pm 0.401^*$
	$Sta$	$20.05 \pm 0.341$	$24.98 \pm 0.455^*$
Proteins (%dw)	$Exp_L$	$60.50 \pm 1.304$	$62.75 \pm 1.421^{ns}$
	$Sta$	$55.78 \pm 1.195$	$59.09 \pm 1.244^*$
Lipids (%dw)	$Exp_L$	$6.58 \pm 0.302$	$3.86 \pm 0.204^*$
	$Sta$	$6.11 \pm 0.151$	$3.58 \pm 0.279^*$

$Exp_L$  and  $Sta$  represent late exponential phase and stationary phase, respectively

“\*” and “ns” refer to significant and insignificant differences, respectively, with the corresponding untreated culture

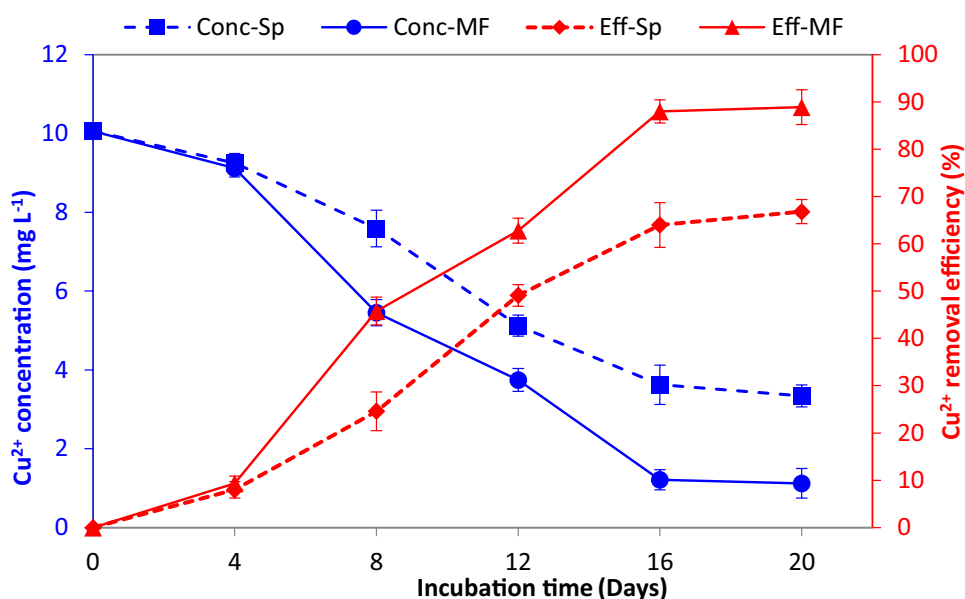
### 3.2 Copper removal

The residual concentrations of  $\text{Cu}^{2+}$  in the medium, as well as the removal efficiencies, were evaluated. The highest significant  $\text{Cu}^{2+}$  removal efficiency of 88.0% was recorded on the 16th day of *S. platensis* incubation under SMF, which was 37.5% higher than the corresponding control (Fig. 4). Therefore,  $\text{Cu}^{2+}$  concentration decreased from  $10 \text{ mg L}^{-1}$  to 1.2 and  $3.6 \text{ mg L}^{-1}$  in SMF-treated and control cultures, respectively. Comparatively, *S. platensis* showed high activity as biosorbent for the  $\text{Cd}^{2+}$  removal by optimization of adsorption conditions including pH, temperature, metal concentration, and contact time [44], where the highest removal efficiency under the optimized conditions was 87.7%. This finding confirms the applicability of SMF as a physical treatment to enhance the biosorption process in microalgae. In order to achieve the maximum biomass productivity and copper removal with a satisfactory cell density, biomass was harvested at the late exponential phase (16th day) and used for further experiments.

### 3.3 Feedstock characterization

Disposed masks were mixed in different ratios with *S. platensis* and used further for Co-HTL. In addition, ultimate and proximate analysis of the blends as well as the TGA was studied. Table 2 shows the ultimate and proximate analysis for the 2 feedstocks as well as the blends. It can be seen that *S. platensis* contains relatively high nitrogen content (9.13 %dw), which decreased by increasing the mask ratio. The high nitrogen content of microalgal biomass is attributed to the high proportion of cellular proteins [45]. Similarly, sulfur showed the same pattern, where the highest sulfur

**Fig. 4** Residual copper concentration (Conc) and copper removal efficiency (Eff) by *Spirulina platensis* grown in synthetic wastewater (Sp) and under static magnetic field (MF). Biomass was harvested on the 16th day for further experiments



content (0.72 %dw) was recorded in *S. platensis*. High nitrogen and sulfur contents in the feedstock result in high N- and S-containing compounds in the bio-oil and, consequently, has negative environmental impacts due to NO<sub>x</sub> and SO<sub>x</sub> emissions [46]. On the other hand, carbon and hydrogen contents were higher in the masks (83.84 and 13.77 %dw, respectively). In addition, masks showed 29.6% higher volatiles than *S. platensis*, which resulted in 94.2% lower ash content (Table 2). Comparatively, Wang et al. [42] recorded 6.5 %dw ash content in *Spirulina* powder, which is 10.3% lower than that recorded in the present study. The relatively high ash content of *S. platensis* in the present study might be attributed to copper accumulation in the biomass through biosorption and using inorganic metals for flocculation during harvest [41, 47]. Thus, masks showed desirable characteristics for high-quality bio-oil production.

TGA showed that decomposition of masks starts at higher temperature (≈330 °C) comparing to *S. platensis*, while full decomposition of masks took place at ≈490 °C (Fig. 5). The thermal decomposition of masks in a single stage is attributed to the mostly presence of C–C bonds that promote random scission mechanism at high temperature [48]. In addition, very low residue was recorded after thermal decomposition of masks, which is in agreement with the proximate analysis. However, high-temperature requirement for mask thermal decomposition is not desirable for bio-oil production due to high energy consumption. Differently, *S. platensis* showed three main decomposition stages, which is the typical pattern for algal biomass [45, 49, 50]. The main biomass decomposition was recorded during the second stage (≈208–400 °C), where the maximum weight loss was recorded due to degradation of most organic compounds. During this stage, the polymeric components of the biomass undergo thermal degradation where weak bonds are broken and more stable/stronger chemical bonds are formed [46, 51]. In the last stage, a very low weight loss can be recorded which is attributed to very slow decomposition of carbonaceous residues [45]. In agreement with the results of proximate analysis, masks showed much lower ash content than *S. platensis*.

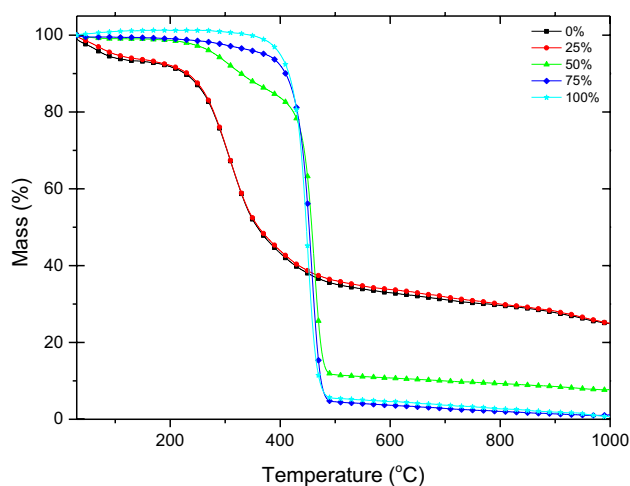


**Fig. 5** Thermogravimetric analysis (TGA) of *Spirulina platensis* (0), disposable masks (100%), and at different mask blend ratios (25%, 50%, and 75%, w/w)

### 3.4 Co-HTL of *S. platensis* and masks

The influence of different mask ratios on the distribution of the main products of Co-HTL with *S. platensis* was studied at different temperatures (Fig. 6). Results showed that increasing temperature for the same feedstock results in reduction of biochar proportion and increase of WSG. For instance, biochar and WSG from HTL of *S. platensis* at 200 °C showed 28.9% and 52.0%, respectively (Fig. 6A). However, increasing temperature to 300 °C (Fig. 6B) and 400 °C (Fig. 6C) resulted in reduction of biochar by 2.4- and 3.8-times, with simultaneous increase in the WSG by 22.4% and 38.5%, respectively, with respect to 200 °C. The same trend was recorded with all feedstock blends (Fig. 6). Thus, increasing of temperature enhanced the conversion rate by reducing biochar yield (Fig. 6). Regarding the bio-oil, the initial increase of temperature to 300 °C led to increase in the bio-oil yield for all feedstocks. However, a further increase to 400 °C reduced bio-oil yield for *S. platensis* while increased it for masks. This finding confirms that high temperature is required for mask decomposition, while is

**Table 2** Ultimate and proximate analysis of *Spirulina platensis* (0), disposed masks (100%), and at different mask blend ratios (25%, 50%, and 75%, w/w)

Mask blend ratio (%)	Ultimate analysis (wt%)					Proximate analysis (wt%)				HHV (MJ kg <sup>-1</sup> )
	N	C	H	S	O	Moisture	Volatile matter	Ash	Fixed carbon	
0	9.13	42.19	5.88	0.72	34.83	5.25	75.25	7.25	12.25	18.95
25	3.16	60.25	11.45	0.34	19.19	4.12	81.12	5.61	9.15	33.11
50	1.91	75.53	12.18	0.13	5.48	3.02	85.96	4.77	6.25	40.45
75	0.37	82.75	12.13	0.00	1.77	1.45	93.45	2.98	2.12	43.09
100	0.00	83.84	13.77	0.00	1.97	0.19	97.54	0.42	1.85	45.46

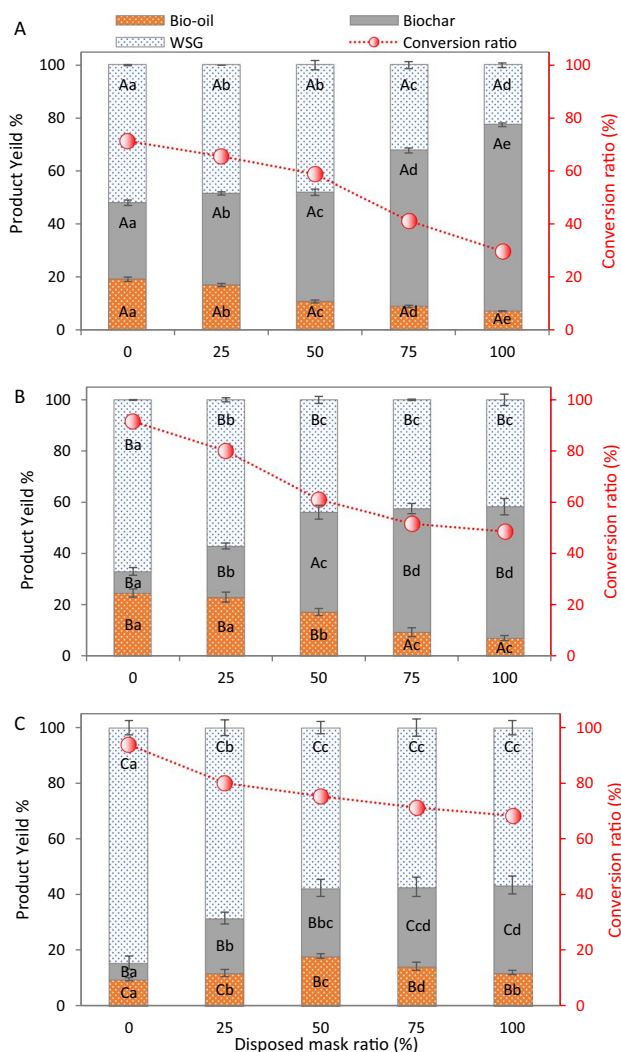


**Fig. 6** Product distribution and conversion ratio from (co-)hydrothermal liquefaction of *Spirulina platensis* (0) with different blend ratios of disposable masks at 200 °C (A), 300 °C (B), and 400 °C (C). WSG refers to gas and water-soluble products. The same small letters in the same series for different feedstocks at the same temperature indicate insignificant differences (at  $P \leq 0.05$ ), while the same capital letters for the same feedstock at different temperature indicate insignificant differences (at  $P \leq 0.05$ )

not desirable for microalgae since it leads to decomposition of condensable products (bio-oil) to syngas. It can be confirmed by the increase of syngas yield from *S. platensis* at 400 °C in favor of bio-oil (Fig. 6C). At different temperatures and blend ratios, the highest bio-oil yield was recorded at 300 °C (Fig. 6B) using *S. platensis* and 25% mask blend ratio (24.6% and 23.0%, respectively, which showed insignificant differences with each other). However, further increase of mask blend ratio to 50% and 75% significantly reduced the bio-oil yield to 17.2% and 9.3%, respectively. Individual HTL of masks at 300 °C showed the lowest bio-oil yield of

7.0%. Therefore, the present results recommend HTL of *S. platensis* or Co-HTL of mask with *S. platensis* at 25% blend ratio from a quantitative aspect.

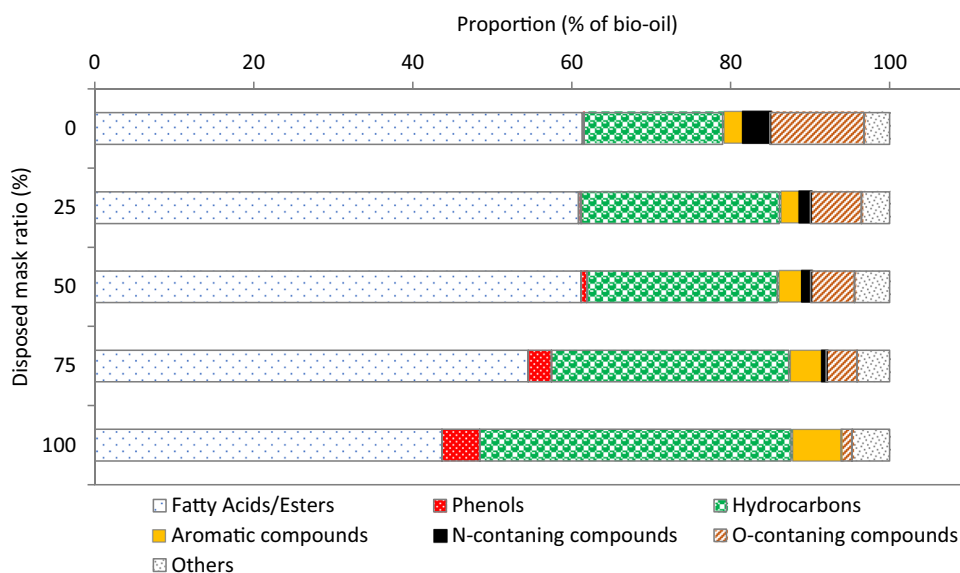
### 3.5 Bio-oil characteristics

The detailed chemical composition of the produced crude bio-oil at different mask blend ratios was further analyzed by GC/MS (Supplementary data, Table S2). It can be noted that the crude bio-oil of different feedstocks is a complex mixture containing many organic compounds within a wide carbon range of C5–C60. Based on the functional groups of the different detected components, they can be classified into seven main groups namely fatty acids/esters, phenols, hydrocarbons, aromatic compounds, nitrogen-containing compounds, oxygen-containing compounds, and traces of other compounds. Figure 7 summarizes the main groups of the bio-oil from HTL of *S. platensis* or masks and Co-HTL at different blend ratios. Results confirmed that the individual HTL of algal biomass showed high proportion of nitrogen- and oxygen-containing compounds (3.6% and 11.9%, respectively), with relatively low aromatic compounds (2.4%) and hydrocarbons (17.4%). Similarly, Tang et al. [52] confirmed that bio-oil from algal thermochemical conversion contains high proportion of nitrogen- and oxygen-containing compounds with lower hydrocarbon content. Introducing masks resulted in significant changes in the bio-oil composition. Mask blend ratio of 25% reduced the nitrogen-containing compounds by 55.6% with respect to HTL of algae. Further increase in mask blend ratio resulted in more reduction in nitrogen-containing compounds, reaching 0% in the bio-oil from individual HTL of masks. These results confirm that masks promote the denitrification reaction of algal biomass during HTL process. In addition, 25% mask blend ratio enhanced the hydrocarbons by 43.7% over the individual microalgae. GC/MS results confirmed a considerable increase in fatty acids/esters at lower mask blend ratios, which decreased at higher ratios owing to the synergistic action of the two used feedstocks during thermal decomposition reaction [21]. Such synergistic action might be attributed to the secondary reactions in the liquefaction reactor and volatile oligomerization during condensation process [53, 54].

In addition to the diverse chemical groups, carbon number can be used to estimate the size of organic molecules in the crude bio-oil and its suitability as a fuel. Figure 8A shows carbon atoms distribution based on the semiquantitative estimation of the identified components. Results confirmed that 25% and 50% mask blend ratios increased the compounds within the carbon ranges C18 and C36. The organic components in the fractionated bio-oil can be



**Fig. 7** The main chemical fractions identified by GC/MS of the bio-oil produced by (co-) hydrothermal liquefaction of *Spirulina platensis* (0) with different blend ratios of disposable masks at 300 °C



divided based on the carbon length into four fuel categories, namely light fuels (less than C5), gasoline (C5–C12), diesel (C13–C24), and heavy oil (more than C24). The latter is a solid structure, starting with paraffin wax, then tar and finally asphaltic bitumen with low economic value. It can be indicated from Fig. 8B that the majority of the compounds from different blend ratios represented the ranges of diesel fuels. *S. platensis* showed relatively higher heavy oil ratio (47.9%), which decreased by increasing the mask blend ratio and reached the minimum value of 16.0% in the bio-oil from individual HTL of masks. In addition, blending of masks with *S. platensis* enhanced the compounds within the diesel range in favor of gasoline and heavy oil. This finding suggests that masks enhanced the compounds with shorter carbon chain in the bio-oil, where the relatively high ash content in *S. platensis* might improve the decomposition of masks [55]. Therefore, Co-HTL of masks with microalgae is an advantageous technique to obtain a wide range of desirable biofuel varieties. Considering all aspects of quantity and quality, 25% blend ratio is suggested to obtain high bio-oil yield with improved quality. In that context, future studies on catalytic Co-HTL of masks with different biomass feedstocks and optimization of liquefaction conditions might further enhance the produced bio-oil to a higher grade.

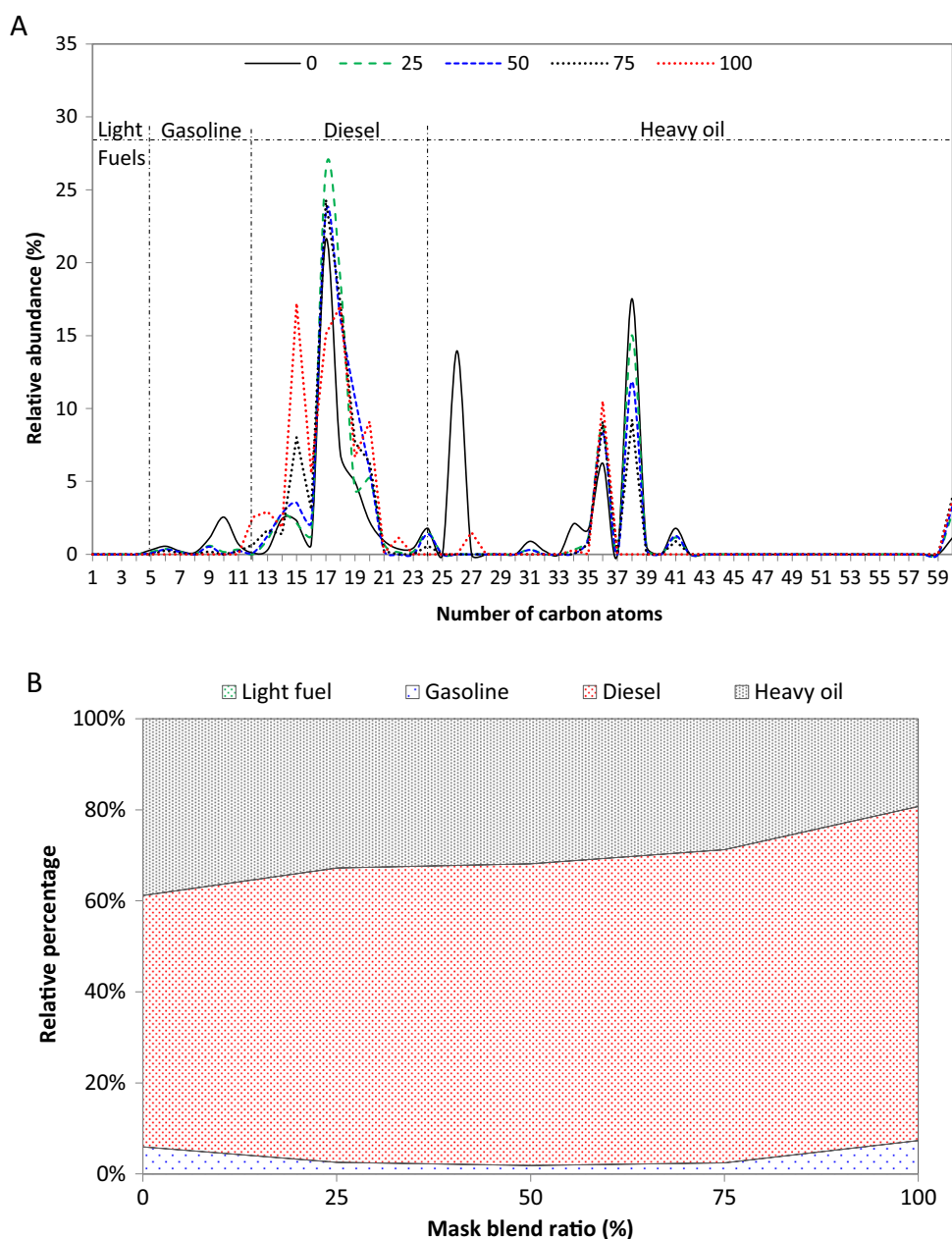
### 3.6 Technical feasibility

Based on microalgal biomass production, bio-oil yield, and the estimated land area for large-scale cultivation, it is possible to evaluate the technical feasibility of the bio-oil produced from Co-HTL of 1-ton feedstock (Table 3). Considering the improved quality of the bio-oil while keeping high yield, 25%

blend ratio is suggested as discussed in Section 3.5. The land area required to grow *S. platensis* and biomass yield was estimated based on the cultivation system used in our previous pilot-scale study [56]. Using the suggested photobioreactor with a total volume of 320 L in a land area of 2.0 m<sup>2</sup>, 70.08 ton ha<sup>-1</sup> y<sup>-1</sup> of areal biomass is estimated to be produced annually. HTL of 1 ton of masks would produce 69.6 kg of bio-oil (Table 3). However, blending of masks with microalgae at 25% (w/w) enhanced the bio-oil yield by 2.3-time (229.6 kg). It is noteworthy to mention that the estimated bio-oil production from blended feedstock in the present study is 86.2% higher than the biodiesel yield from microalgal biomass (123.3 g kg<sup>-1</sup>) using the same cultivation system [56]. This finding confirms the superiority of thermochemical conversion of the whole feedstock over biodiesel recovery from the lipidic portion of the biomass.

In addition to high-quality bio-oil production through mask blending with *S. platensis*, its cultivation could adsorb 6.2 kg of Cu<sup>2+</sup> per ton of biomass produced, i.e., 4.7 kg at the suggested blend ratio (Table 3). Considering average copper concentration of 119.98 µg L<sup>-1</sup> in the global river and lake water bodies during the 2010s [57], production of 1 ton *S. platensis* could treat about 51,675 m<sup>3</sup> of copper-contaminated wastewater. Interestingly, blending of waste masks with microalgae at 25% would simultaneously reduce the land area required for microalgae cultivation. According to a recent report [58], the global demand for disposable face masks was estimated at 129 billion masks per month to protect public health amid COVID-19. Assuming an average mask weight of 3.21 g as detected in the present study, the estimated global mask waste could be 4.97 × 10<sup>6</sup> ton year<sup>-1</sup>. According to the China State Council [59], the total land area of China is 9.6 × 10<sup>8</sup> ha. Using the suggested

**Fig. 8** Relative distribution (by relative peak area) based on carbon atoms numbers in the bio-oil obtained by (co-) hydrothermal liquefaction of *Spirulina platensis* (0) with different blend ratios of disposable masks at 300 °C (A), and the relative percentage of different fuel categories based on the ranges of carbon atoms (B)



system, only 0.02% of the land area in China can produce sufficient *S. platensis* biomass ( $1.49 \times 10^7$  ton) to convert all the global disposed masks through Co-HTL at a 25% mask blend ratio, with an estimated crude bio-oil yield of

$4.56 \times 10^6$  ton year<sup>-1</sup>. Thus, the present study suggested a simple and practical approach for efficient waste mask recycling coupled with wastewater treatment for improved crude bio-oil production.

**Table 3** Technical feasibility of bio-oil production from (co-) hydrothermal liquefaction of disposed masks, and at mask blend ratios of 25% (w/w) at 300 °C using estimated feedstock of 1 ton

Mask blend ratio (%)	Bio-oil yield (%)	<i>S. platensis</i> amount (ton)	Required area for <i>S. platensis</i> ( $\times 10^{-3}$ ha)	Bio-oil production (kg)	Cu removal (kg) <sup>a</sup>
25% blend	22.96	0.75	3.01	229.6	4.7
Masks	6.96	0	0.00	69.6	0.0

<sup>a</sup>Based on 6.2 mg g<sup>-1</sup> dw Cu<sup>2+</sup> removal in the present study

## 4 Conclusions

The present study confirmed the potential of *S. platensis* grown under SMF for Cu<sup>2+</sup> biosorption. From quantitative and qualitative aspects, results showed that Co-HTL of microalgae at 25% (w/w) mask blend ratio is a desirable route for bio-oil production. The highest significant bio-oil yield was recorded by HTL at 300 °C for *S. platensis* and 25% mask blend ratio. Results confirmed that individual HTL of algal biomass results in bio-oil with high proportion of nitrogen-containing compounds (3.6%). However, the 25% mask blend ratio reduced the nitrogen-containing compounds by 55.6%. In addition, blending of masks with *S. platensis* enhanced the hydrocarbons and compounds within the diesel range in favor of gasoline and heavy oil. Overall, Co-HTL of masks with microalgae is a good choice to enhance bio-oil production using wet biomass with a wide range of desirable biofuel varieties. As the whole world looks forward to a post-COVID-19 future, it is of great importance to ensure hygiene and safe management of the disposed masks. More investments and proper policies must take care on management of such wastes at the same level of public health and infection control.

**Supplementary Information** The online version contains supplementary material available at <https://doi.org/10.1007/s13399-021-01891-2>.

**Acknowledgements** This work was financially funded by the National Natural Science Foundation of China (52050410328), start-up funds for high-end talents of Chengdu University (No. 2081920048), and Chengdu University 2021 Student Incubation and Cultivation Program (CDU\_CX\_2021379). ZhiXue team thanks Ms. Lihong Zhang (Chengdu Diweilepu Technology Co., Ltd.) for providing help to perform the required analysis.

## References

- World Health Organization (2021) WHO Coronavirus (COVID-19) Dashboard. <https://covid19.who.int/>. Accessed 27 Apr 2021
- Das O, Neisiany RE, Capezza AJ et al (2020) The need for fully bio-based facemasks to counter coronavirus outbreaks: a perspective. *Sci Total Environ* 736:139611. <https://doi.org/10.1016/j.scitotenv.2020.139611>
- Singh N, Tang Y, Zhang Z, Zheng C (2020) COVID-19 waste management: effective and successful measures in Wuhan, China. *Resour Conserv Recycl* 163:105071
- Wang MW, Cheng YR, Ye L et al (2020) The COVID-19 outbreak: the issue of face masks. *Infect Control Hosp Epidemiol* 41:974–975
- Adyel TM (2020) Accumulation of plastic waste during COVID-19. *Science* 369:1314–1315
- van Doremalen N, Bushmaker T, Morris DH et al (2020) Aerosol and surface stability of SARS-CoV-2 as compared with SARS-CoV-1. *N Engl J Med* 382:1564–1567. <https://doi.org/10.1056/nejmc2004973>
- Kampf G, Todt D, Pfaender S, Steinmann E (2020) Persistence of coronaviruses on inanimate surfaces and their inactivation with biocidal agents. *J Hosp Infect* 104:246–251
- Sangkham S (2020) Face mask and medical waste disposal during the novel COVID-19 pandemic in Asia. *Case Stud Chem Environ Eng* 2:100052. <https://doi.org/10.1016/j.cscee.2020.100052>
- Jung S, Lee S, Dou X, Kwon EE (2021) Valorization of disposable COVID-19 mask through the thermo-chemical process. *Chem Eng J* 405:126658. <https://doi.org/10.1016/j.cej.2020.126658>
- Aragaw TA (2020) Surgical face masks as a potential source for microplastic pollution in the COVID-19 scenario. *Mar Pollut Bull* 159:111517. <https://doi.org/10.1016/j.marpolbul.2020.111517>
- Pereira de Albuquerque F, Dhadwal M, Dastyar W et al (2021) Fate of disposable face masks in high-solids anaerobic digestion: experimental observations and review of potential environmental implications. *Case Stud Chem Environ Eng* 3:100082. <https://doi.org/10.1016/j.cscee.2021.100082>
- World Health Organization (2020) Health-care waste. <https://www.who.int/news-room/fact-sheets/detail/health-care-waste>. Accessed 22 Apr 2021
- Dharmaraj S, Ashokkumar V, Pandiyan R et al (2021) Pyrolysis: an effective technique for degradation of COVID-19 medical wastes. *Chemosphere* 275:130092
- Ghodrat M, Rashidi M, Samali B (2017) Life cycle assessments of incineration treatment for sharp medical waste. In: Zhang L et al (eds) *Energy technology 2017. The minerals, metals & materials series*. Springer, Cham. [https://doi.org/10.1007/978-3-319-52192-3\\_14](https://doi.org/10.1007/978-3-319-52192-3_14)
- Wang J, Shen J, Ye D et al (2020) Disinfection technology of hospital wastes and wastewater: suggestions for disinfection strategy during coronavirus disease 2019 (COVID-19) pandemic in China. *Environ Pollut* 262:114665
- Wu SL, Kuo JH, Wey MY (2019) Thermal degradation of waste plastics in a two-stage pyrolysis-catalysis reactor over core-shell type catalyst. *J Anal Appl Pyrolysis* 142:104641. <https://doi.org/10.1016/j.jaap.2019.104641>
- Lee S, Cho AR, Park D et al (2019) Reusable polybenzimidazole nanofiber membrane filter for highly breathable PM 2.5 dust proof mask. *ACS Appl Mater Interfaces* 11:2750–2757. <https://doi.org/10.1021/acsami.8b19741>
- Abnisa F, Daud WMAW (2014) A review on co-pyrolysis of biomass: an optional technique to obtain a high-grade pyrolysis oil. *Energy Convers Manag* 87:71–85
- Uzoejinwa BB, He X, Wang S et al (2018) Co-pyrolysis of biomass and waste plastics as a thermochemical conversion technology for high-grade biofuel production: recent progress and future directions elsewhere worldwide. *Energy Convers Manag* 163:468–492
- Abomohra AE-F, Sheikh HMA, El-Naggar AH, Wang Q (2021) Microwave vacuum co-pyrolysis of waste plastic and seaweeds for enhanced crude bio-oil recovery: experimental and feasibility study towards industrialization. *Renew Sustain Energy Rev* 149:111335. <https://doi.org/10.1016/j.rser.2021.111335>
- Uzoejinwa BB, He X, Wang S et al (2020) Co-pyrolysis of seaweeds with waste plastics: modeling and simulation of effects of co-pyrolysis parameters on yields, and optimization studies for maximum yield of enhanced biofuels. *Energy Sources, Part A Recover Util Environ Eff* 42:954–978
- Guerin M, Huntley ME, Olaizola M (2003) *Haematococcus astaxanthin*: applications for human health and nutrition. *Trends Biotechnol* 21:210–216
- Almomani F, Judd S, Bhosale RR et al (2019) Intergraded wastewater treatment and carbon bio-fixation from flue gases using *Spirulina platensis* and mixed algal culture. *Process Saf Environ Prot* 124:240–250. <https://doi.org/10.1016/j.psep.2019.02.009>
- Shao W, Ebaid R, El-Sheekh M et al (2019) Pharmaceutical applications and consequent environmental impacts of *Spirulina* (Arthrospira): an overview. *Grasas Aceites* 70:292

25. Luo L, He H, Yang C et al (2016) Nutrient removal and lipid production by *Coelastrella* sp. in anaerobically and aerobically treated swine wastewater. *Bioresour Technol* 216:135–141. <https://doi.org/10.1016/j.biortech.2016.05.059>
26. Zhai J, Li X, Li W et al (2017) Optimization of biomass production and nutrients removal by *Spirulina platensis* from municipal wastewater. *Ecol Eng* 108:83–92. <https://doi.org/10.1016/j.ecoleng.2017.07.023>
27. Abomohra AE-F, Jin W, Tu R et al (2016) Microalgal biomass production as a sustainable feedstock for biodiesel: current status and perspectives. *Renew Sustain Energy Rev* 64:596–606
28. Abomohra AE-F, El-Hefnawy ME, Wang Q et al (2021) Sequential bioethanol and biogas production coupled with heavy metal removal using dry seaweeds: towards enhanced economic feasibility. *J Clean Prod* 316:128341. <https://doi.org/10.1016/j.jclepro.2021.128341>
29. Abomohra, Zheng X, Wang Q et al (2021) Enhancement of biodiesel yield and characteristics through in-situ solvo-thermal co-transesterification of wet microalgae with spent coffee grounds. *Bioresour Technol* 323:124640
30. Barreiro DL, Prins W, Ronsse F, Brilman W (2013) Hydrothermal liquefaction (HTL) of microalgae for biofuel production: state of the art review and future prospects. *Biomass Bioenerg* 53:113–127
31. Aiba S, Ogawa T (1977) Assessment of growth yield of a blue—green alga, *Spirulina platensis*, in axenic and continuous culture. *Microbiology* 102:179–182
32. Shao W, Ebaid R, Abomohra AE, Shahan M (2018) Enhancement of *Spirulina* biomass production and cadmium biosorption using combined static magnetic field. *Bioresour Technol*. <https://doi.org/10.1016/j.biortech.2018.06.009>
33. Abomohra AE-F, Wagner M, El-Sheekh M, Hanelt D (2013) Lipid and total fatty acid productivity in photoautotrophic fresh water microalgae: screening studies towards biodiesel production. *J Appl Phycol* 25:931–936. <https://doi.org/10.1007/s10811-012-9917-y>
34. Payne JK, Stewart JR (1988) The chemical composition of the thallus wall of *Characiosiphon rivularis* (Characiosiphonaceae, Chlorophyta). *Phycologia* 27:43–49
35. Kochert G (1978) Carbohydrate determination by the phenol sulfuric acid method. In: Hellebust JA, Craigie JS (eds) *Handbook of phycollogical methods: physiological and biochemical methods*. Cambridge University Press, London, pp 95–97
36. Bradford MM (1976) A rapid and sensitive method for quantitation of microgram quantities of protein utilizing the principle of protein-dye binding. *Anal Biochem* 72:248–254
37. Abomohra AE-F, Jin W, El-Sheekh M (2016) Enhancement of lipid extraction for improved biodiesel recovery from the biodiesel promising microalga *Scenedesmus obliquus*. *Energy Convers Manag* 108:23–29
38. Noll CA, Betz LD (1952) Determination of copper ion by a modified sodium diethyldithiocarbamate procedure. *Anal Chem* 24:1894–1895. <https://doi.org/10.1021/ac60072a008>
39. Sossella F, Rempel A, Monroe Araújo Nunes J et al (2020) Effects of harvesting *Spirulina platensis* biomass using coagulants and electrocoagulation–flotation on enzymatic hydrolysis. *Bioresour Technol* 311:123526. <https://doi.org/10.1016/j.biortech.2020.123526>
40. ASTM (2006) Standard test methods for analysis of wood fuels. American Society for Testing and Materials, West Conshohocken
41. Wang S, Yerkebulan M, Abomohra AEF et al (2019) Microalgae harvest influences the energy recovery: a case study on chemical flocculation of *Scenedesmus obliquus* for biodiesel and crude bio-oil production. *Bioresour Technol* 286:121371
42. Wang H, Tian W, Zeng F et al (2020) Catalytic hydrothermal liquefaction of *Spirulina* over bifunctional catalyst to produce high-quality biofuel. *Fuel* 282:118807. <https://doi.org/10.1016/j.fuel.2020.118807>
43. Yuan C, Wang S, Cao B et al (2019) Optimization of hydrothermal co-liquefaction of seaweeds with lignocellulosic biomass: merging 2nd and 3rd generation feedstocks for enhanced bio-oil production. *Energy* 173:413–422
44. Al-Homaidan AA, Alabdullatif JA, Al-Hazzani AA et al (2015) Adsorptive removal of cadmium ions by *Spirulina platensis* dry biomass. *Saudi J Biol Sci* 22:795–800. <https://doi.org/10.1016/j.sjbs.2015.06.010>
45. Wang S, Uzoejinwa BB, Abomohra AE-F et al (2018) Characterization and pyrolysis behavior of the green microalga *Micractinium conductrix* grown in lab-scale tubular photobioreactor using Py-GC/MS and TGA/MS. *J Anal Appl Pyrolysis* 135:340–349
46. Wang S, Zhao S, Uzoejinwa BB et al (2020) A state-of-the-art review on dual purpose seaweeds utilization for wastewater treatment and crude bio-oil production. *Energy Convers Manag* 222:113253
47. Cao B, Wang S, Hu Y et al (2019) Effect of washing with diluted acids on *Enteromorpha clathrata* pyrolysis products: towards enhanced bio-oil from seaweeds. *Renew Energy* 138:29–38. <https://doi.org/10.1016/j.renene.2019.01.084>
48. Kim H-S, Kim S, Kim H-J, Yang H-S (2006) Thermal properties of bio-flour-filled polyolefin composites with different compatibilizing agent type and content. *Thermochim Acta* 451:181–188
49. Cao B, Sun Y, Guo J et al (2019) Synergistic effects of co-pyrolysis of macroalgae and polyvinyl chloride on bio-oil/bio-char properties and transferring regularity of chlorine. *Fuel* 246:319–329. <https://doi.org/10.1016/j.fuel.2019.02.037>
50. Azizi K, Moraveji MK, Najafabadi HA (2017) Characteristics and kinetics study of simultaneous pyrolysis of microalgae *Chlorella vulgaris*, wood and polypropylene through TGA. *Bioresour Technol* 243:481–491
51. El-Sayed SA, Mostafa ME (2014) Pyrolysis characteristics and kinetic parameters determination of biomass fuel powders by differential thermal gravimetric analysis (TGA/DTG). *Energy Convers Manag* 85:165–172
52. Tang Z, Chen W, Hu J et al (2020) Co-pyrolysis of microalgae with low-density polyethylene (LDPE) for deoxygenation and denitrification. *Bioresour Technol* 311:123502
53. Butler E, Devlin G, Meier D, McDonnell K (2013) Fluidised bed pyrolysis of lignocellulosic biomasses and comparison of bio-oil and micropyrolyser pyrolysate by GC/MS-FID. *J Anal Appl Pyrolysis* 103:96–101
54. Patwardhan PR, Dalluge DL, Shanks BH, Brown RC (2011) Distinguishing primary and secondary reactions of cellulose pyrolysis. *Bioresour Technol* 102:5265–5269
55. Yang J, Rizkiana J, Widayatno WB et al (2016) Fast co-pyrolysis of low density polyethylene and biomass residue for oil production. *Energy Convers Manag* 120:422–429
56. Abomohra AEF, El-Sheekh M, Hanelt D (2014) Pilot cultivation of the chlorophyte microalga *Scenedesmus obliquus* as a promising feedstock for biofuel. *Biomass Bioenergy* 64:237–244. <https://doi.org/10.1016/j.biombioe.2014.03.049>
57. Zhou Q, Yang N, Li Y et al (2020) Total concentrations and sources of heavy metal pollution in global river and lake water bodies from 1972 to 2017. *Glob Ecol Conserv* 22:e00925. <https://doi.org/10.1016/j.gecco.2020.e00925>
58. Prata JC, Silva ALP, Walker TR et al (2020) COVID-19 pandemic repercussions on the use and management of plastics. *Environ Sci Technol* 54:7760–7765. <https://doi.org/10.1021/acs.est.0c02178>
59. China State Council (2017) Notice of the state council on issuing the outline of the national land planning (2016–2030). <http://www.gov.cn/>

**Publisher's note** Springer Nature remains neutral with regard to jurisdictional claims in published maps and institutional affiliations.